A COMPARISON OF CUMULUS PARAMETERIZATION
SCHEMES IN THE WRF MODEL

Erin K. Gilliland and Clinton M. Rowe *
University of Nebraska, Lincoln, Nebraska

1. INTRODUCTION

The new Weather Research and Forecasting model (WRF), like other numerical models, can make use of several cumulus parameterization schemes (CPS). The purpose of this study is to determine how the available CPSs in the WRF model simulate summertime convection. Summertime convection was chosen in order to determine the skill of these CPSs in representing warm-season convective events, which have been shown by Wang and Seamen (1997) to be represented less accurately than cold-season events. This is because the dominant large-scale dynamic forcing during the cold-season events are modeled more accurately than the strong thermal forcing at the surface that are more prominent in warm-season events. Also, during the warm season, prediction of convection and rainfall may vary due to the different timing and location of initial convection determined by each CPS. In order to understand the impact of the differences in the CPSs, the three available CPSs in the WRF model are used to simulate a warm-season convective system. Both idealized simulations and a single warm-season event are examined and the simulated precipitation distribution, intensity and detailed structure are analyzed. The objective is to compare the differences among precipitation forecasts using the different CPSs in the WRF model, not to judge which CPS is better or worse than the others.

2. METHODOLOGY

2.1 Numerical model

The horizontal resolution of the WRF model can range from meters to tens of kilometers and the domain can range from tens to thousands of kilometers. Current CPSs were developed for grid scales of 32 to 48 km (Arakawa 2004). However, the current versions have been shown to work well

at a 12 km grid scale (Wang and Seaman 1997), but the WRF model targets grid scales between 1 km and 10 km (Skamarock et al. 2005). Current CPSs were not developed for such fine grid scales. A model running at a fine grid scale, such as 4 km, can resolve some (but not all) mesoscale processes and the CPS may not work as well or might not be needed.

Currently, the Advanced Research WRF (ARW, version 2.1.1) supports three separate CPSs: the Kain-Fritsch (Kain and Fritsch 1990, 1993; Kain 2004) and Betts-Miller-Janjic (Betts and Miller 1993; Janjic 1994) schemes and the Grell-Devenyi ensemble scheme (Grell and Devenyi 2002). Each of the schemes has been developed from older and less complicated parameterization schemes and has been modified based on testing from previous model simulations. To compare the differences among the three CPSs, both idealized and real-case simulations are preformed over a set time period utilizing the same initial and boundary conditions for each CPS and then the model output is compared. In addition, a simulation without a CPS was performed to determine if the model could simulate the convection explicitly.

2.2 Idealized modeling

To compare the CPSs in a controlled environment, an idealized case was chosen. To test the skill of the available CPSs, the three-dimensional supercell case supplied with the WRF distribution is employed. Supercells tend to occur more frequently during the warmer months and this corresponds to the time period when CPSs have been shown to be less effective. Also, supercells are mesoscale features that models and CPSs often have difficulty representing accurately.

The three-dimensional supercell test case uses standard idealized modeling specifications. To represent microphysics, Kessler's warm rain physics scheme is employed. The model assumes no surface fluxes or frictional effects and does not account for radiation. Using simple physics will isolate the effects of the CPS and not

* Corrresponding author address: Clinton M. Rowe, Dept. of Geosciences, Univ. of Nebraska, Lincoln, NE 68588-0340; e-mail: crowe1@unl.edu.

be dependent on the other physics schemes available. The idealized case simulates a domain with constant, one-dimensional temperature and wind profiles as initial conditions and open lateral boundary conditions. The sounding is based on the thermodynamic profile used by Weisman and Klemp (1982) to model severe storms, including supercells. This profile represents an environment that has CAPE of 2200 J kg^{-1}, which represents moderate instability. Also the sounding has moist conditions starting at 850 hPa and extending into the upper troposphere. To represent the wind conditions and vertical shear, a quarter circle hodograph is used. This wind profile has been shown to produce the most "classic" looking supercells (Weisman and Rotunno 2000). The thermodynamic profile sets up the initial environment and an initial temperature perturbation is then placed in the domain to trigger convection and develop the initial updraft of the supercell. This temperature perturbation is a bubble with a maximum of 3K centered in the domain with the temperature perturbation decreasing linearly over a horizontal radius of 10 km and a vertical radius of 1500 m. These initial conditions are used for all idealized model simulations.

The original three-dimensional supercell case provided in the WRF model has a horizontal resolution of 2 km and a 500 m vertical resolution. The domain is 80 km east-west, 80 km north-south, and 20 km vertically. At this resolution, the model should be able to resolve convection explicitly. To investigate the use of the CPSs, a 4 km horizontal resolution is used in the present study and the domain was increased to 160 km by 160 km to visualize the entire life cycle of the storm. The WRF model was first run at 4 km horizontal resolution without a CPS to determine if the convection could be rewsolved explicitly at this resolution. Next, runs with each of the three available CPSs were undertaken determine if they would enhance the 4 km output or are not needed. The results of these four simulations can then be compared to the original 2 km simulation without a CPS.

2.3 Warm-season convective case study

The warm-season convective system chosen for this study occurred on 28-29 July 2005 in South Dakota and Nebraska. This case was chosen to represent an isolated convective system that produced supercells and severe weather in parts of central Nebraska. For the 28-29 July 2005 case, the domain is 1200 km by 1200 km centered just south of the Nebraska/South Dakota border. For this case study, the external data are from the North American Regional Reanalysis (NARR) dataset for both the initial conditions for the domain and the lateral boundary conditions, at three-hour intervals, for the entire time period of the case study. A fixed field NARR data file is also used to define the land mask, vegetation type, soil type, surface slope and soil characteristics (Mesinger et al. 2006).

The length of the real-case simulations was 36 hours to include 12 hours of spin-up time followed by 24 additional hours to simulate the forecast period. The domain and model attributes used for the real case are summarized in Table 1.

3. IDEALIZED SIMULATIONS

For all of the idealized simulations conducted, rain mixing ratio, vertical velocity and winds at 3 km above ground level (AGL) were used to determine storm structure and strength. At 3 km AGL, the strength of the updraft and downdraft of the system are best represented, for both stages of the supercell, single and split. Above 3 km AGL the environmental winds become overpowering and they do not interact with the storm to show the mid-level rotation that is characteristic of a supercell. Also, in order to examine the storm system after the main supercell splits; a level that is far enough below the anvil's height is needed to compare the left and right moving supercells. Below 3 km the rain water mixing ratios and vertical velocities are weaker and won't give as good as a representation of the storm structure.

Horizontal grid spacing	4 km
Number of horizontal grid points	300
Time step	12 s
Number of vertical levels	31
Vertical spacing	log p
Top of model	100 hPa
Initial conditions	NARR
Lateral boundary conditions	NARR
Microphysics	WSM6
Planetary boundary layer	Yonsei University
Surface layer	5-layer soil model
Shortwave radiation	Dudhia (1989)
Longwave radiation	RRTM

Table 1: Domain and model specifications for real case simulations.

This level coincides with previous work by Weisman and Rutonno (2000), who use 3 km AGL to study the strength and dynamics of supercells.

3.1 Simulation results

The results of running the idealized supercell case at a 4 km grid spacing with no CPS indicate that the WRF model at horizontal resolutions around 4 km can resolve convection explicitly, at least for this idealized case. The classic supercellular characteristics (*i.e.,* split into two cells, mid-level rotation and pronounced hook) were modeled successfully (Fig. 1). The no-CPS simulation was able to initiate the main updraft, then represent the split of that main updraft into right- and left-moving supercells. After the split, the right-moving supercell continued to grow in strength and produced severe storm characteristics such as a hook and mid-level rotation. The left-moving supercell also continued to grow and produce significant amounts of rain. By 105 minutes, the storm started taking on the characteristics of a quasi-linear structure. These features are similar to the results produced by the original 2 km supercell case, giving support to the idea that a CPS may not be needed at a 4 km grid spacing.

The storm structure that results from using the Kain-Fritsch (KF) scheme is similar to the structure simulated without a CPS (Fig. 1), again representing the key features of an idealized supercell. One advantage of the scheme compared to not using a CPS is the continued support of the middle updraft at 105 minutes. Due to its use of more complicated microphysics, KF was able to represent sub-grid scale features of the updraft and rain processes. This representation of sub-grid scale features makes the KF scheme more realistic and possibly beneficial for real-time modeling.

The Betts-Miller-Janjic (BMJ) scheme, like the no-CPS and KF scheme, was able to represent the key supercell features at a grid spacing of 4 km (Fig. 1), but their development was delayed compared to the other simulations and BMJ did not develop a third cell. This scheme did not produce as much rain water as the previous simulations, resulting in weaker downdrafts. Moisture in the environment is an important variable in the BMJ scheme and even though the sounding has a deep moist layer, the BMJ scheme is not able to realize this moisture in the form of precipitation.

When the 4 km idealized supercell case is run the Grell-Devenyi (GD) ensemble scheme, the updraft only exists for 30 minutes then all of the rain water is removed and the updraft ceases to exist (Fig. 1). The GD ensemble scheme is not able to handle convection at 4 km, without modification to the code (Wei Wang, personal communication).

3.2 Comparison and discussion

An important feature of a supercell is the updraft. The updraft is needed to transport warm moist air into the supercell; therefore, accurate representation of vertical velocities in the model is essential. Since all of the simulations (2 and 4 km) showed the split of the main updraft, the maximum upward vertical velocities at 3 km AGL for the right- and left-moving supercells are examined (Fig. 2). For these idealized simulations, the clockwise, quarter-circle shaped hodograph used favors the right-moving supercells such that, immediately after the split of the main updraft, the right updraft should be stronger than the left. The time series of upward velocities for the right storm (Fig. 2a) shows that the 4 km no-CPS case has the same tendencies as the 2 km original case with an almost steady difference of
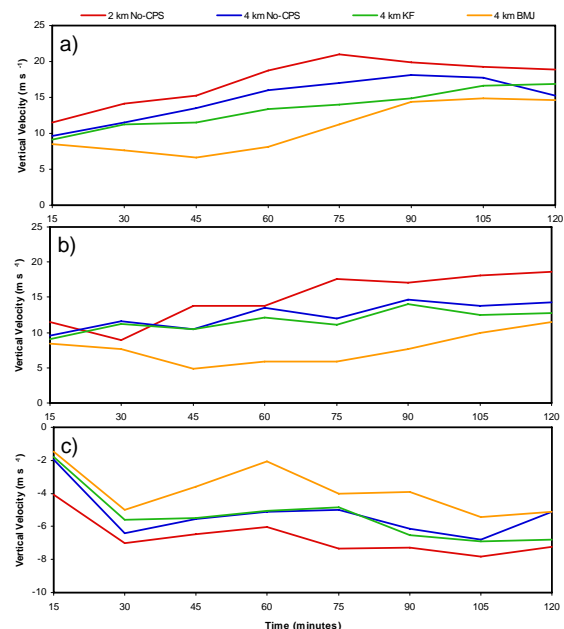

Fig. 2. Maximum vertical velocities (m s^{-1}) for the four simulations. a) upward velocities for the right-moving supercell, b) upward velocities for the left-moving supercell, c) downward velocities.
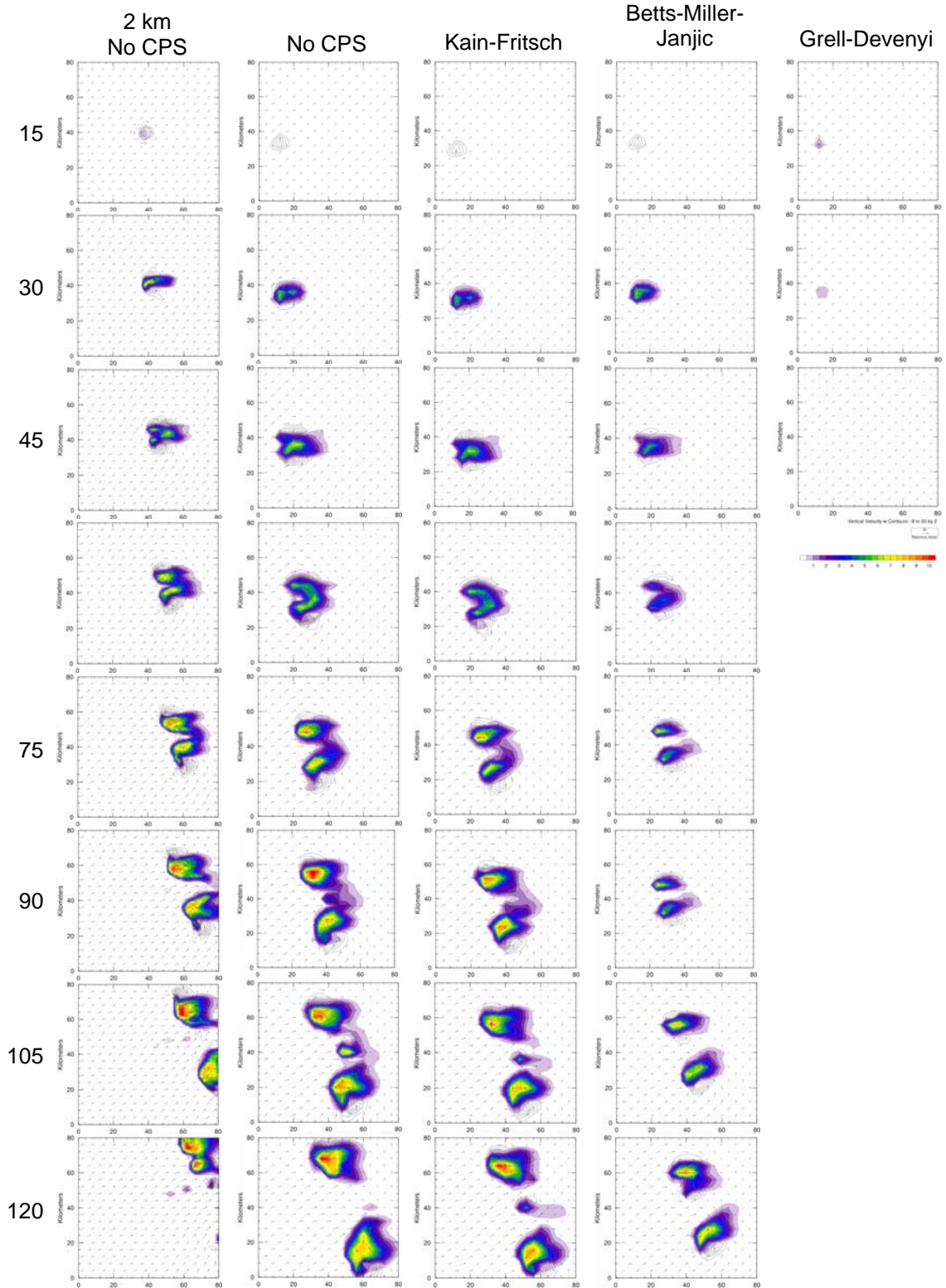
Fig. 1. Storm structure at 3 km AGL for the idealized supercell case. Vertical velocities are contoured at 2 m s^{-1} intervals with negative values dashed and a maximum value of 20 m s^{-1}. Rain mixing ratio (g kg^{-1}) is shaded. Winds are depicted with a reference vector magnitude of 20 m s^{-1}. Time (min) is noted along the left side and the simulations are noted across the top.

4 m s^{-1}. Upward velocities in the KF simulation have a similar shape to the no-CPS cases, with a difference of roughly 7 m s^{-1} difference from the 2 km no-CPS simulation. The case using the BMJ scheme, unlike the KF simulation, does not follow the same trend as the no-CPS simulations. It is only able to produce maximum upward velocities that are similar to the other model runs after 90 minutes. This inability to produce stronger upward velocities could be caused by the adjustment process itself. When the BMJ scheme attempts to adjust the model sounding to a predetermined reference profile the amount of latent heat released may not be sufficient to produce a realistic initial updraft for a supercell. The KF scheme on the other hand, uses CAPE that is present in the sounding to determine storm properties such as heating and moistening. This method does produce updraft characteristics that are consistent with, although somewhat weaker than, the 2 km idealized simulation with explicit convection.

For the left-moving supercell (Fig. 2b), the simulations using no CPS and the KF scheme follow the same pattern and are nearly equal in magnitude throughout the entire time period. By 45 minutes the left moving supercell is apparent and becoming more intense (Fig. 1). Maximum updraft velocities follow the same up/down pattern of the 2 km no-CPS case, except there is a time lag. This lag appears because all of the 4 km idealized model runs simulate the split of the storm 45 minutes after initiation while the 2 km simulations show the split after 30 minutes. This is most likely due to the size of the initial perturbation. For the 2 km simulations the initial perturbation, which has a radius of 10 km, at the center of the domain takes up 10 grid spaces. The same size perturbation is used in the 4 km simulations and fills only 5 grid spaces maximum. Other than the lag due to splitting, the 4 km simulations with no CPS and the KF CPS produce similar results for the left moving supercell. However, as with the right-moving supercell, the BMJ scheme simulates weaker vertical velocities for the left-moving supercell than the other simulations.

In addition to buoyancy created by latent heat release during convection, convergence near the surface can have an impact on the magnitude of upward vertical motion. At 45 minutes, both the no-CPS simulation (not shown) and the KF simulation (Fig. 3) have two low pressure centers that relate to the left- and right-moving storms.

The pressure gradients thus produced cause an increase in wind speed upwind of the storm. This increase in wind speed causes a speed convergence near the perturbation and might be the main source for upward motion at the two flanks. The BMJ simulation, on the other hand, has a weak pressure gradient on the right flank and lacks any significant gradient on the left flank (Fig. 3). This small gradient has very little effect on the winds and there is minimum speed convergence in the lower levels. By 90 minutes the BMJ simulation shows convergence near the right-moving storm, as for the KF simulation (Fig. 3), and this corresponds to an increase in upward velocities (Fig. 2). The BMJ left-moving storm at 90 minutes still has weaker updrafts than do the other simulations, possibly due to the lack of convergence in the lower-levels near the storms updraft. Finally at 105 minutes (Fig. 3) both simulations show convergence at 750 m and this corresponds to an increase in upward velocity in the BMJ simulation (Fig. 2). Thus, one common feature among the simulations is the presence of low-level convergence and the increase in upward velocities. The explicit convection and the KF scheme, unlike the BMJ scheme, are able to reproduce the low-level convergence early in the life of the supercell, which is a key factor in forecasting and modeling supercells and convective systems because of its effect on the strength of the updraft.

The KF and no-CPS simulations at 4 km have maximum downdraft velocities similar to those of the 2 km simulation with magnitudes only 1.0 to 1.5 m s^{-1} smaller (Fig. 2). Downdraft velocities in the BMJ simulation, as with the updrafts, differ from the other simulations during most of the time period.

Overall, idealized modeling of a classic three-dimensional supercell at 4 km grid spacing has demonstrated that convection at this resolution can be resolved without a CPS, at least for this case. If either the Kain-Fritsch or Betts-Miller-Janjic CPS is used in the WRF model, convection will be present but may be misrepresented. The best option at 4 km may be not to use a CPS since the WRF model was able to resolve the main features of the supercell and simulate an environment similar to that which was modeled at 2 km, where a CPS is not needed.
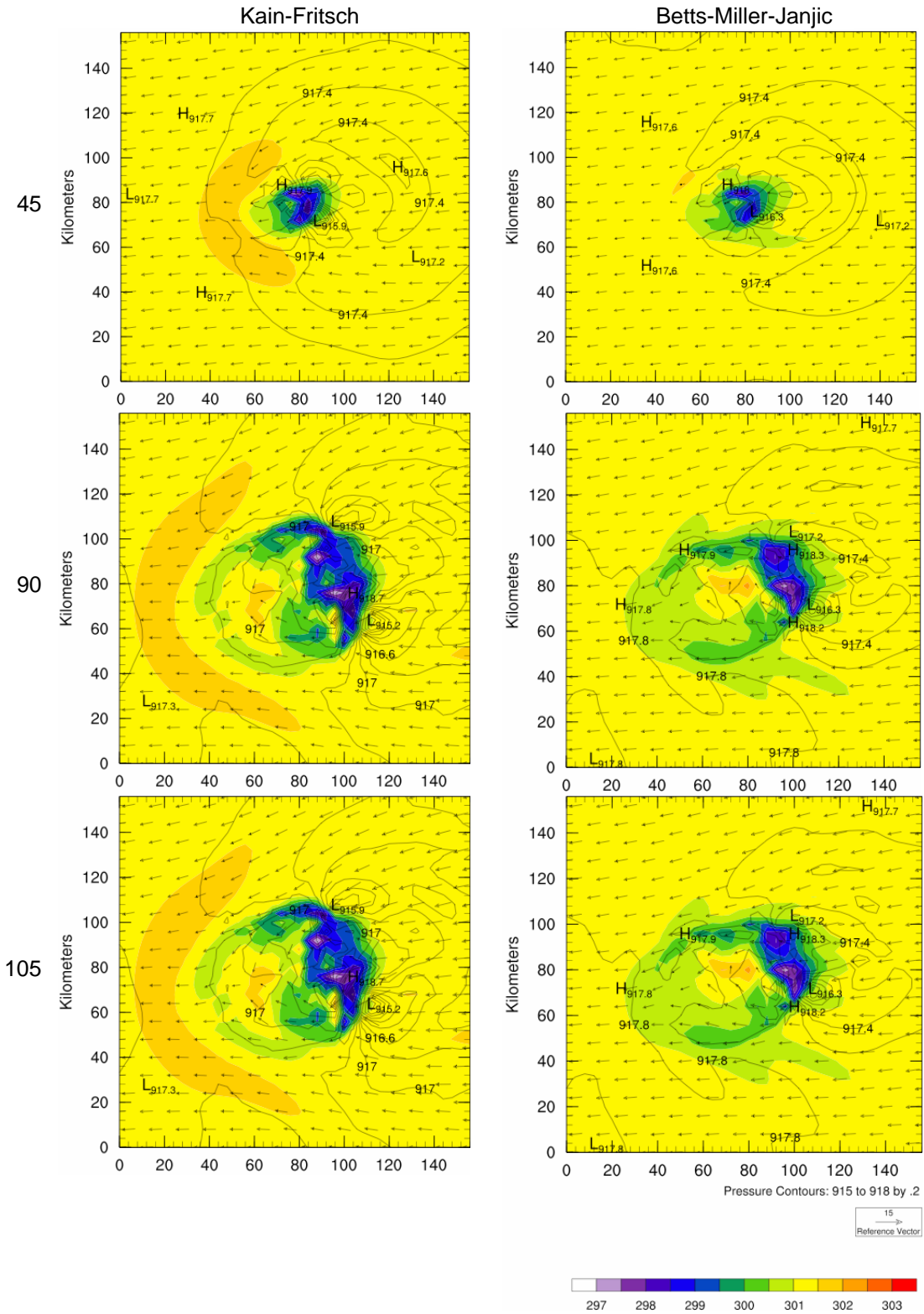
Fig. 3. Storm structure at 750 m, with potential temperature (K) shaded and pressure (hPa) contoured, for the Kain-Fritsch (left) and Bette-Miller-Janjic (right) simulations. Winds are in m s^{-1} and time (min) is noted along the left side.

4. REAL-CASE SIMULATIONS

4.1 Synoptic setting

At 1800 UTC 28 July 2005, approximately 3 hours before the start of localized convection, high pressure is centered over southeastern Kansas and there is a shortwave upper-level feature i present at 250 hPa which has moved downstream into the southern region of the domain (Fig. 4). A tongue of high θ_e (> 330 K) is present in the western part of domain with an steep gradient along the South Dakota/Nebraska border. By 1800 UTC a deformation zone has developed in north-central Nebraska, causing the strongest confluence to be in northeastern Nebraska and western Wyoming. Due largely to daytime heating, surface-based CAPE is 800-1200 J kg^{-1}. Surface observations show a meridional temperature gradient across South Dakota and a moisture gradient in western Nebraska.

Between 2000 and 2100 UTC, small areas of convection started to develop in central Nebraska (Figure 5). The convection is initiated by weak and mostly unchanged large-scale forcings from earlier in the day. The persistent high pressure is able to maintain southerly winds over the domain throughout the lower-levels and to advect moisture into the domain from the Gulf of Mexico. It is at 2100 UTC, when the region of high θ_e has the steepest gradient along the South Dakota/Nebraska border (Fig. 4), that convection is well-supported. Also, the deformation zone has shifted northward into South Dakota and the strongest confluence is along the borders of Nebraska, Wyoming and South Dakota. Surface-based CAPE continues to increase and has a maximum between 1200-1400 J kg^{-1} in the northwestern corner of Nebraska. A strong temperature gradient remains in place along the western border of the Dakotas and a strong moisture gradient exists in western Nebraska and eastern Wyoming. A wind maximum of approximately 10 m s^{-1} exists in the southwestern corner of Nebraska and northwestern Kansas.

Overall, the large-scale forcing for convection is weak or ill-defined. There was no significant frontal passage or upper-level trough to provide a large area of lift. However, a colder air mass did extend into the domain and, together with southerly flow from the high pressure, created a deformation zone/region of confluence and this stationary front became a source for lift. This boundary remained stationary through the initiation and early development of the convection. The high pressure in the southeastern portion of the domain was a key factor in producing the strong gradient of low-level θ_e and advecting moisture northward into the region. Since this case took place at the end of July, daytime solar heating was strong, warming the ground significantly and causing an increase in positive buoyancy.

4.2 Results

For this case study, all of the precipitation simulated in the region of interest (South Dakota and Nebraska) was convective in nature (i.e., no explicit precipitation was produced by the model). This indicates that only the CPSs were producing precipitation, not the microphysics.

During storm initiation and early development (1800 UTC to 0200 UTC), the no-CPS simulation was unable to represent the isolated convective cells and the resulting precipitation, confirming that the precipitation was convective in nature and occurred at scales smaller than 4 km; thus, it is unable to be represented without the use of a CPS. As with the no-CPS simulation, the BMJ simulation is unable to represent any significant convective precipitation. A pre-storm model sounding (1800 UTC), characteristic of the region where convection is first observed near Rapid City, South Dakota has dry air aloft as well as in the lowest 200 hPa. However it lacks the deep moist layer necessary for the BMJ scheme to produce convective precipitation. Since the BMJ scheme depends on a deep layer of available moisture, its effectiveness is limited in a region with little moisture even when moderate CAPE is available. Since neither the no-CPS nor the BMJ simulations produced any significant precipitation, the results from these simulations will not be discussed further.

4.2.1 Kain-Fritsch

The KF simulation starts producing convective precipitation at 1800 UTC (Fig. 5) on the lee side of the Black Hills. This area provides some key ingredients for convection: winds sheared by the terrain, moisture advected from the south, an elevated LCL and moderate CAPE. However, radar does not show any precipitation around the Black Hills prior to 1800 UTC.

Since the KF scheme is dependent on the amount of CAPE, it continues to trigger convection
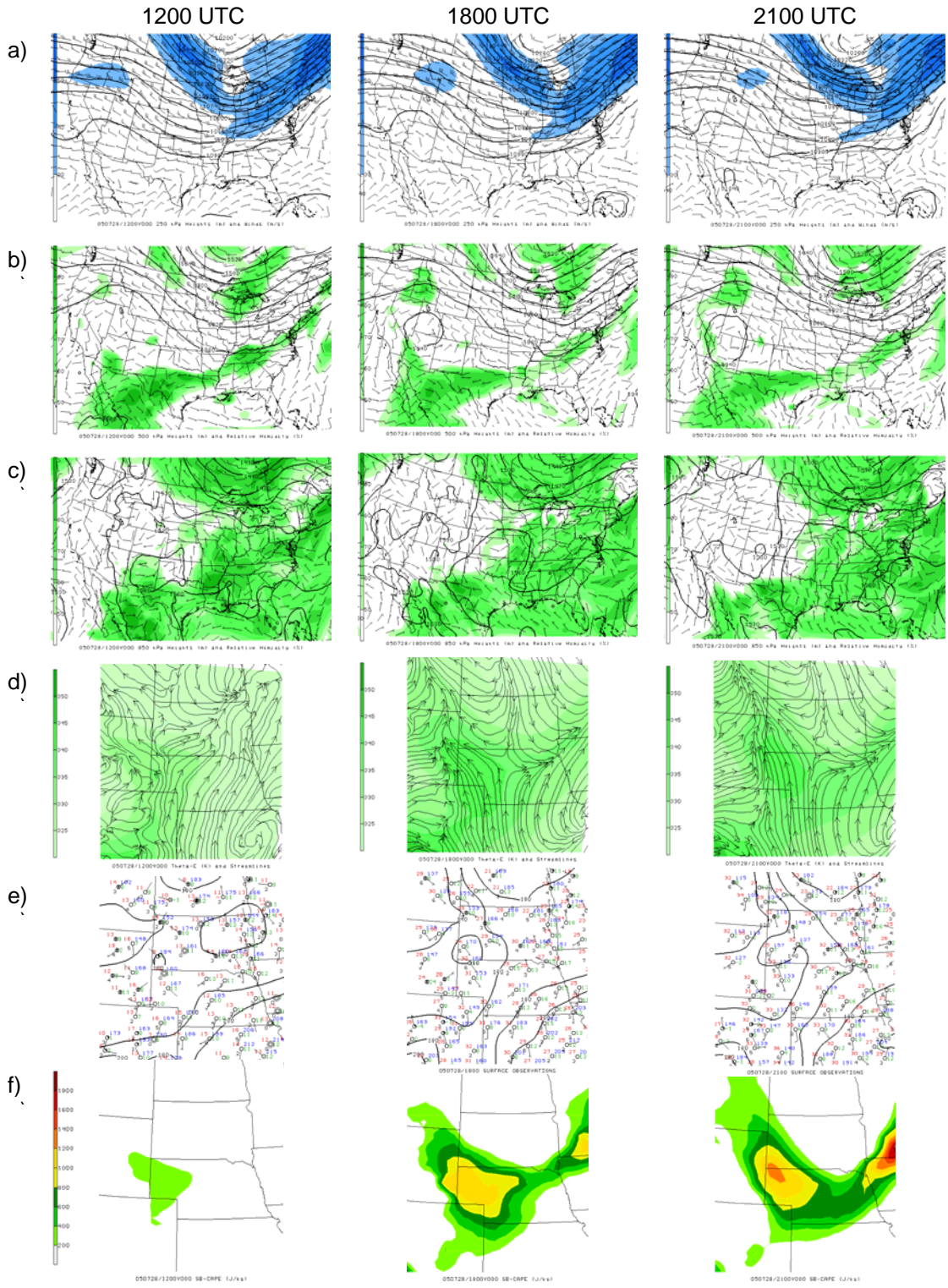
Fig. 4. Synoptic setting on 28 July 2005. a) 250 hPa height contoured every 60 m with wind speed shaded, b) 500 hPa height contoured every 60 m with relative humidity shaded, c) 850 hPa height contoured every 30 m with relative humidity shaded, d) surface streamlines with equivalent potential temperature (K) shaded, e) surface observations with pressure contoured every 2 hPa, and f) surface-based CAPE (J kg^{-1}). Temperatures are in °C, all winds are in m s^{-1}, and times are denoted across the top.
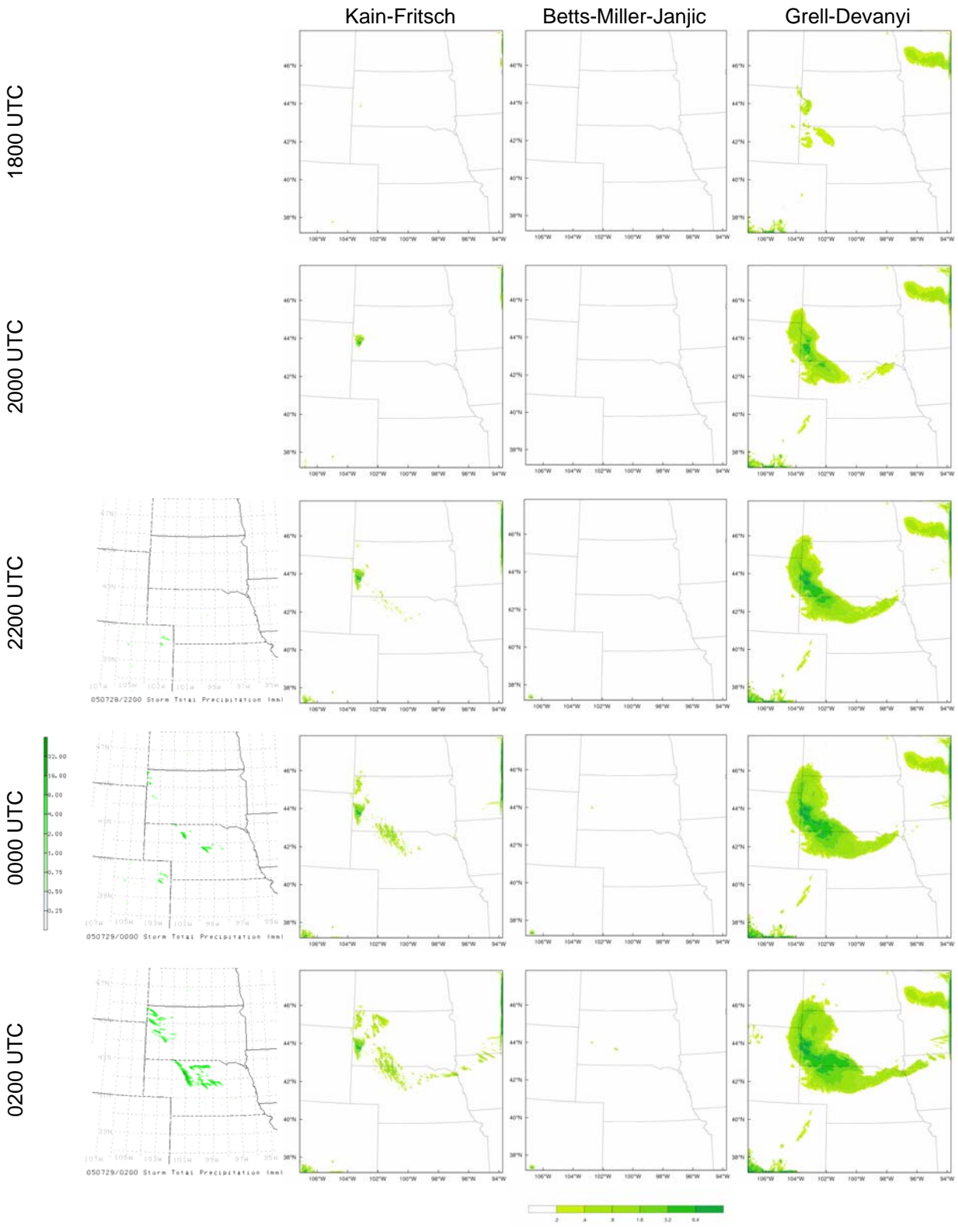
Fig. 5. Total precipitation (mm) for 28-29 July 2005. Radar-based storm total precipitation (left column) is shown only for times following observed convective initiation. Times are noted along the left and simulations are noted across the top.

as long as there is CAPE present. This causes the isolated area of precipitation in southwestern South Dakota (Fig. 5) to expande 2000 UTC. Once the scheme is triggered, the KF scheme employs a cloud model to simulate the effects of clouds and their thermodynamic properties. This scheme allows heat and water vapor to be entrained into the updraft, which is beneficial for this case because of the dramatic θ_e gradient adjacent to the convective region. As the KF scheme is able to entrain the higher θ_e air from the south into the area with moderate values of CAPE the effectiveness of the updraft to produce precipitation is enhanced. However, as was the case at 1800 UTC, radar does not show any rainfall across the domain at 2000 UTC. Still, the KF scheme only shows the continued development of the precipitation region in western South Dakota that was initiated two hours earlier and it has not triggered convection elsewhere in the domain.

At 2200 UTC, the KF scheme continues to produce precipitation along the border of Nebraska and South Dakota (Fig. 5). The model soundings at the locations with the most precipitation simulated by the KF scheme (43°N, 101.5°W; and 42.5°N, 101°W) contain moderate CAPE (1500-1700 J kg^{-1}) and are mostly dry, although they are relatively moist between 500 hPa and are nearly saturated around 650 hPa. Due to past convection, the KF profiles are being modified and are able to continue producing precipitation. The moisture tendency from the scheme is preconditioning the environment for convection, which is allowing the KF simulation to continue producing precipitation in this region. With the exception of the early storm in southwestern South Dakota, the KF scheme is able to simulate the timing of the storm fairly well, with convection starting in Nebraska around 2200 UTC and then developing in northwestern South Dakota by 0000 UTC.

At 0200 UTC convection is simulated from the KF scheme in northeastern Nebraska (Fig. 5). It is in this area that northerly winds in western South Dakota and southerly winds in Nebraska continue to form a convergence zone. The KF scheme is able to produce precipitation with the abundant moisture in this area plus lift provided by the convergence zone.

4.2.2 Grell-Devenyi

The GD simulation triggers convection at 1700 UTC (not shown) and by 1800 UTC a widespread area of convective precipitation is present in western South Dakota (Fig. 5). An area of precipitation in western Nebraska was produced by GD earlier in the day (1200 UTC), which may have assisted in the earlier initiation of convection in the GD simulation by providing an additional source of moisture. However, it can not be excluded that other dynamic controls, such as moisture convergence, in GD ensemble members could have triggered convection.

At 2000 UTC, when the KF scheme has produced only a isolated areas of precipitation, the GD simulation has a wider/longer swath of precipitation along the South Dakota/Wyoming border and into northwestern Nebraska (Fig. 5). Also, by this time convection has developed in northeastern Nebraska along another dew-point gradient (Fig. 4). This region is also experiencing confluence due to a deformation zone along the border of Nebraska and South Dakota. The GD scheme has used the moisture and lift in the environment to trigger new convection and precipitation in this area. For the rest of the simulation (Fig. 5) the GD scheme continues to produce precipitation in the same area as the KF scheme but is unable to simulate the isolated nature of the convection.

4.3 Discussion

Representation of the 28-29 July 2005 summertime convective case by the WRF model differed significantly depending on the choice of convective scheme. When deciding which CPS to choose, it is important to know what type of convective system is likely to develop, how the CPS could handle the synoptic and mesoscale system and the type of environment (dry/moist). For this case, at a grid spacing of 4 km the simulation with no-CPS was unable to represent any precipitation, even with favorable atmospheric conditions. Therefore this case, which lacks any major synoptic forcing, apparently requires a CPS to represent the sub-grid scale convection and precipitation.

As for the choice of CPS, the model was run with the three available schemes: the Betts-Miller-Janjic scheme, Kain-Fritsch scheme and the Grell-Devenyi ensemble. The BMJ simulation was never able to produce precipitation. As with the

no-CPS simulation, favorable atmospheric conditions existed that, with other schemes, was able to produce precipitation. A key issue for the BMJ scheme was the lack of moisture in the soundings. For the BMJ scheme to produce precipitation, the relaxation of the profiles to pre-determined reference profiles has to dry and warm the environment. The environmental profiles of the domain are already dry and warm which limits the effectiveness of the scheme.

The KF scheme on the other hand was able to account of the small-scale processes that lead to the development of convection. The scheme initiated convection due to the presence of moderate CAPE and convection was sustained by employing a more complicated static control to represent updrafts. The static control was able to account for the advection of high θ_e air into the region and incorporate its contribution to the moisture field. The feedback from the scheme enhanced and preconditioned the environment, allowing for a relatively accurate representation of the isolated convective cells and their resulting precipitation.

Like the KF simulations, the GD ensemble was able to detect the development of convection. The weakness of the GD scheme was in its early triggering of convection and development of a broad area of convection that is not representative of the actual isolated nature of the convective cells. Overall, it was able to represent the general area and intensity of precipitation.

5. SUMMARY

Simulations using the WRF model provide insight into the effectiveness of cumulus parameterization schemes in representing isolated convection at various grid spacings. Idealized modeling demonstrates that, at a fine resolutions such as 2 or 4 km, classic supercellular convective features including a reflectivity hook, mid-level rotation and storm splitting can be resolved explicitly and a CPS is not needed. The Kain-Fritsch and Betts-Miller-Janjic schemes also were able to trigger convection at 4 km, however the resulting vertical velocities and rain mixing ratios were smaller in magnitude than the no-CPS simulation. The BMJ simulation especially had difficulty representing vertical velocities accurately. This could be due to the early release of latent heat and the resulting struggle to regain values similar to the other simulations. Another possibility is the lack of low-level convergence to support the

continued growth of the initial and split updraft. The Grell-Devenyi ensemble scheme is currently unable to handle idealized convection at small grid spacings. Possible modification to the code could alleviate this problem but this was not undertaken for this study. These simulations demonstrated that caution must be used when employing a CPS.

There are two main conclusions resulting from the simulations for the 28-29 July 2005 case study. First, it is not always appropriate to assume that model simulations using small grid spacings (< 5 km) will not need a CPS. Depending on the strength of the synoptic-scale forcing and time of year, certain atmospheric settings warrant the use of a cumulus parameterization scheme to represent the effects of sub-grid scale convective processes. The convective system on 28-29 July 2005 is an example of an environment that needs a CPS to represent accurately the small sub-grid scale processes that occur with isolated, discrete convective cells. The atmospheric setting of this case made representation of precipitation challenging and it was shown that the model could not represent, even with a complicated microphysics package, the convection explicitly. Secondly, a strong limitation of the Betts-Miller-Janjic scheme is its strong dependence on available moisture. While Janjic (1994) made improvements to the original Betts-Miller scheme to make it more applicable to non-tropical convection, its simple representation of cloud processes still apparently limit in its effectiveness in certain environments.

6. ACKNOWLEDGEMENTS

7. REFERENCES

Arakawa, A., 2004: The cumulus parameterization problem: Past, present, and future. *J. Climate,* 17, 2493-2525.

Betts, A. K., and M. J. Miller, 1993: The Betts-Miller scheme. *The Representation of Cumulus Convection in Numerical Models, Meteor. Monogr.,* No. 24, Amer. Meteor. Soc., 107-121.

Grell, G. A., and D. Devenyi, 2002: A generalized approach to parameterizing convection combining

ensemble and data assimilation techniques. *Geophys. Res. Lett.,* **29**, 1693-1696.

Janjic, Z. I., 1994: The step-mountain eta coordinate model: Further development of the convection, viscous sublayer, and turbulence closure schemes. *Mon. Wea. Rev.,* **122**, 927-945.

Kain, J. S., 2004: The Kain-Fritsch convective parameterization: An update. *J. Appl. Meteor.,* **43**, 170-181.

Kain, J. S., and J. M. Fritsch, 1990: A one-dimensional entraining/detraining plume model and its application in convective parameterization. *J. Atmos. Sci.,* **47**, 2784-2802.

Kain, J. S., and J. M. Fritsch, 1993: Convective parameterization for mesoscale models: The Kain-Fritsch scheme.   *The Representation of Cumulus Convection in Numerical Models, Meteor. Monogr.,* No. 24, Amer. Meteor. Soc., 165-170.

Mesinger, F., et al., 2006: North American Regional Reanalysis, *Bull. Amer. Meteor. Soc.,* **87**, 343-360.

Skamarock, W. C., J. B. Klemp, J. Dudia, D. O. Gill, D. M. Barker, W. Wang, and J. G. Powers, 2005: A description of the Advanced Research WRF version 2. NCAR Tech. Note, NCAR/TN-468+STR, 88pp.

Wang, W., and N. L. Seaman, 1997: A comparison study of convective parameterization schemes in a mesoscale model. *Mon. Wea. Rev.,* **125**, 252-278.

Weisman, M. L., and J. B. Klemp, 1982: The dependence of numerically simulated convective storms on vertical wind shear and buoyancy. *Mon. Wea. Rev.*, **110**, 504-520.

Weisman, M. L., and R. Rotunno, 2000: The use of vertical wind shear versus helicity in interpreting supercell dynamics. *J. Atmos. Sci.,* **57**, 1452-1472.